# Quasideuteron model for the $(p,d)$ reaction at intermediate energies

B. K. Jain*
*Nuclear Physics Division, Bhabha Atomic Research Centre, Bombay 400085, India*
*and Institute für Theoretische Physik der Universität Heidelberg,*
*D-6900 Heidelberg, Federal Republic of Germany*

(Received 30 June 1982)

The $(p,d)$ reaction at intermediate energies is described in terms of the free $pd$ scattering at backward angles: The formalism is given in the distorted wave approximation. The general features of the cross section, like the angular distribution, the variation with incident energy, and the distribution with respect to momentum transfer, are well accounted for by the predictions of the model.

[NUCLEAR REACTIONS Quasideuteron, $(p,d)$ reaction, intermediate energies, distorted waves.]

## I. INTRODUCTION

The success of the $(p,d)$ reaction at low energies[1] in exploring the single neutron aspect of the nucleus has led, in recent years, to the measurement on the same reaction at higher energies (200–800 MeV) (Refs. 2–4). This reaction, in the pickup model [Fig. 1(a)], apart from measuring the spectroscopic factor, explores the momentum component of the neutron wave function in the nucleus corresponding to the momentum transfer $\vec{Q}=\vec{k}_p-\vec{k}_d$. The higher energy data, therefore, are expected to extend this information, which is limited at lower energies to lower momentum components ($Q \lesssim 200$ MeV/$c$), to higher momentum components ($200 \lesssim Q \lesssim 800$ MeV/$c$). However, because of the involvement of the high momentum transfer, it is not quite certain if the reaction mechanism at these energies would be confined only to the one-nucleon pickup mechanism or would it involve two nucleons. In addition, even if the "one-nucleon" mechanism is enough, there are grave doubts about the description of the neutron, in such a high momentum domain, as a particle moving in an average single-particle potential.[5] Nevertheless, calculations have been done in the distorted wave Born approximation of the pickup mechanism. The results of these calculations, depending upon the choice of the distorting potentials for protons and deuterons and the bound-state wave function for neutrons, vary a great deal in magnitude (one order) and shape.[3,6,7] For a particular choice of these parameters, of course, Shepard and Rost[7] have been successful in explaining the data on $^{16}O(d,p)^{17}O$ at 698 MeV incident energy. On the other hand, in the experimental studies of the $(p,\pi^+)$ and $(p,d)$ reactions, in the similar range of momentum transfer, it has been observed that these two classes of reactions are very similar.[8] The similarity, in fact, is to such an extent that it is possible to successfully describe the $(p,d)$ reaction in terms of the $(p,\pi^+)$ reaction.[9] This suggests that, just like in the $(p,\pi^+)$ and $(p,\gamma)$ reactions, in the $(p,d)$ reaction too it should be important to include the mesonic and baryonic degrees of freedom. With this in mind Boudard *et al.*[6] have analyzed the $^{16}O(d,p)$ data at 698 MeV incident energy in terms of the rescattering diagram similar to that shown in Fig. 1(a) for the $(p,d)$ reaction. This diagram involves the participation of two nucleons in the nucleus through the baryonic excitation of one nucleon and its subsequent deexcitation through its interaction with another nucleon.

Generally speaking the results of this calculation are of a similar quality as that of the conventional DWBA calculations. However, this calculation may be open to criticism because it is not clear to what extent it includes the contribution due to single nucleon pickup (or stripping) in the diagram of Fig. 1(a). This contribution, as suggested by the DWBA calculations, may be quite significant. In this paper we follow a semiphenomenological approach. This approach, which originates from the following observation on the free $pd$ scattering at backward angles, like Boudard *et al.*,[6] involves two nucleons from the nucleus at the interaction vertex. In the $p+d \rightarrow p+d$ scattering at intermediate energies ($E_p > 300$ MeV) it is found that for the successful description of the angular distribution of protons at backward angles (or equivalently the deuteron at forward angles, i.e., $120° < \theta_p \leq 180°$ or $0° \leq \theta_d < 40°$), one must include, in addition to the neutron exchange diagram [Fig. 1(b)], the rescattering diagram of the type shown in Fig. 1(b) (Ref. 10). Comparing these diagrams with those in Fig. 1(a)

 

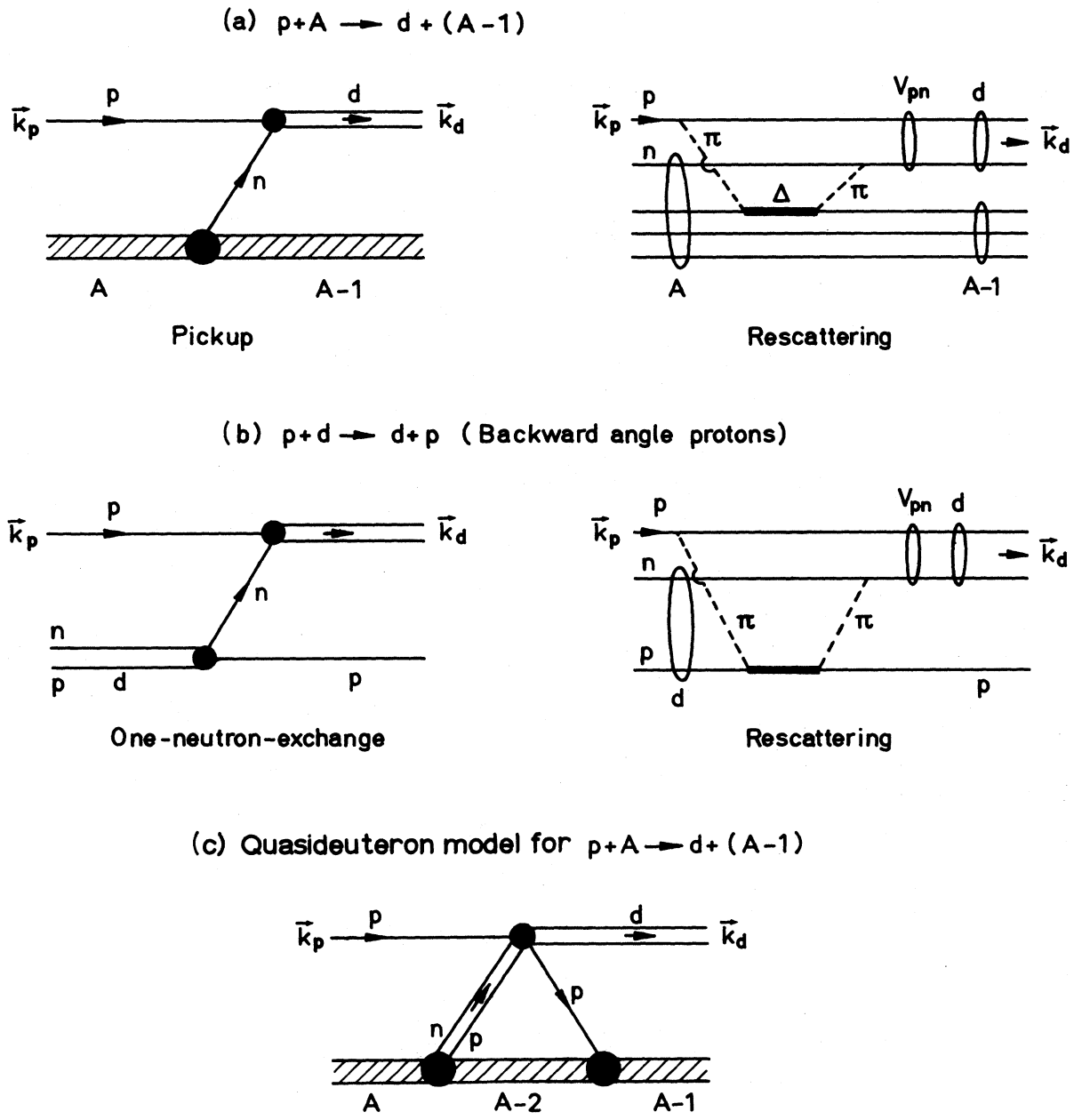


FIG. 1. Interaction graphs.

for the $A(p,d)B$ reaction we find that they are completely analogous. Taking advantage of this similarity, we describe the interaction vertex for the $A(p,d)B$ reaction in terms of that for the $p(d,p)d$ scattering [Fig. 1(c)]. This kind of approach has been used in the past by Källne *et al.*[4] and others[11] for the preliminary analysis of the $^4$He$(p,d)$ data. In this description, out of the two protons and a neutron participating at the vertex, one proton is captured back by the nuclear core and the remaining one with the neutron goes out as a deuteron. The residual nucleus may be left in the one-neutron hole states, coupled to the unexcited or excited proton states of the nucleus. Thus the energy spectrum of the detected deuteron may be much richer in this picture than that in the conventional pickup model. The interaction of the continuum proton and deuteron with the $(A-2)$ core is described by the distorted waves. Since we are interested in the intermediate energy induced $(p,d)$ reaction, these distort-

ed waves are described in the eikonal approximation.

In this paper we derive the expression for the cross section for the $A(p,d)B$ reaction in terms of the quasideuteron vertex. This expression, as we shall see later, in the energy region of interest ($>200$ MeV), apart from the kinematic factor, factorizes into the free $pd$ scattering cross section at backward angles and a nuclear structure factor [Eqs. (24) and (25)], i.e.,

$$\frac{d\sigma}{d\Omega} \propto (\text{kin fac})\sigma_{pd}(\epsilon_L,\theta_p^{\text{c.m.}}) \mid F_l^{BA}(\vec{Q}) \mid^2 , \quad (1)$$

where $\sigma_{pd}$ is the free $pd$ scattering cross section at the appropriate energy and angle. $F^{BA}(\vec{Q})$ is the "distorted" nuclear structure factor, which contains the information about the proton excitation and the neutron hole in the nucleus. The formalism is presented in Sec. II and its predictions are discussed and compared with the experimental data in Sec. III. However, before we go over to the actual formalism in the next section, it may be mentioned that, due to the importance of only high momentum components in the backward $pd$ scattering, the validity of the quasideuteron model does not require that the $np$ pair in the nucleus exist as a deuteron all the time. It is sufficient if it behaves as a deuteron at a short distance, for which there are ample indications.[12]

## II. FORMALISM

The differential cross section for the $A(p,d)B$ reaction in the center-of-mass system is given by

$$\frac{d\sigma}{d\Omega} = F_K \overline{\sum} \mid T_{BA}(\vec{k}_d,\vec{k}_p) \mid^2 , \quad (2)$$

where the kinematic factor $F_K$ is

$$F_K = (2\pi\hbar^2)^{-2} E_p E_A E_d E_B E_c^{-2} (k_d/k_p) . \quad (3)$$

$\overline{\sum}$ represents the appropriate sum and average over the final and initial states, respectively. The transition matrix $T_{BA}$ in the distorted wave approximation has the form

$$T_{BA}(\vec{k}_d,\vec{k}_p) = \int d\vec{k}'_p \int d\vec{k}'_d \chi^*_{\vec{k}'_d}(\vec{k}'_d) \langle B,d,\vec{k}'_d \mid T \mid A,p,\vec{k}'_p \rangle \chi^+_{\vec{k}'_p}(\vec{k}'_p) . \quad (4)$$

Here $\chi$'s are the "distorted waves." They describe the relative motion of the proton and deuteron with respect to the initial and final nuclei with asymptotic center-of-mass momenta $\vec{k}_p$ and $\vec{k}_d$, respectively. $E_x$, in Eq. (3), is the total energy of the particle $x$ and $E_c$ ($=E_p+E_A=E_d+E_B$) is the total energy in the center of mass. The remaining factor in Eq. (4) is the matrix element of the interaction causing the event, taken between the internal states of the colliding pairs. In the quasideuteron model [Fig. 1(c)], this factor is given by

$$\begin{aligned} \langle B,d,\vec{k}'_d \mid T \mid A,p,\vec{k}'_p \rangle &\equiv G(\vec{k}'_d,\vec{k}'_p) \\ &= \left\langle \psi_B(\xi,i)\psi_d^* \left| \sum_{ij} T_p(i,j) \right| \psi_p\psi_A \mid (\xi,i,j) \right\rangle . \end{aligned} \quad (5)$$

Here $i$ denotes protons and $j$ denotes neutrons in the nucleus. $\xi$ stands for the spectator $(A-2)$ nucleons. In order to simplify the treatment of $G$, initially we treat neutrons and protons separately and define an overlap integral for neutrons

$$\langle \psi_{BN}(\xi_N) \mid \psi_{AN}(\xi_N,j) \rangle = \zeta_{BA}(\alpha_n)\psi_{\alpha_n}(j) , \quad (6)$$

where $\psi_{BN}$ ($\psi_{AN}$) is the neutron wave function for the nucleus $B$ ($A$). $\psi_{\alpha_n}(j)$ is the wave function of the $j$th neutron in the nucleus. $\zeta_{BA}(\alpha_n)$ is the normalization constant for $\psi_{\alpha_n}$ and is related to the spectroscopic factor through

$$S_{BA}(\alpha_n) = N \mid \zeta_{BA}(\alpha_n) \mid^2 . \quad (7)$$

Here $N$ is the "active" number of neutrons in a particular "shell" in the target nucleus. Now using Eqs. (6) and (7) and considering that the transition operator $T_p(i,j)$ in Eq. (5) does not depend upon the neutron variables in the final nucleus, we integrate over them. This yields

$$G(\vec{k}'_d,\vec{k}'_p) = S_{BA}^{1/2}(\alpha_n) \left\langle \psi_{BP}(\xi_p,i)\psi_d \left| \sum_i T_p(i,1) \right| \psi_p\psi_{\alpha_n}(1)\psi_{AP}(\xi,i) \right\rangle . \quad (8)$$

In arriving at expression (8), by using the indistinguishability of active neutrons we have removed the sum over $j$ and replaced the $j$th neutron by the first. Like $\psi_{BN}(\psi_{AN})$, $\psi_{BP}(\psi_{AP})$ is the proton wave function for the residual (target) nucleus. At this stage we now invoke that the neutrons and protons in the target nucleus are,

in fact, not completely uncorrelated. At short relative distances they are correlated and these correlations are very much similar to those in a free deuteron. With this observation, for which there are ample indications in the literature,[12] and writing the wave functions in momentum space, we get

$$G(\vec{k}'_d,\vec{k}'_p)=S_{BA}^{1/2}(\alpha_n)\sum_i \int d\xi_p d\vec{k}_1 d\vec{k}_i d\vec{k}'_i \psi^*_{BP}(\xi,\vec{k}'_i)\langle \vec{k}'_i,\vec{k}'_d\phi_d \mid T_p(i,1)\mid \vec{k}'_p,\vec{K}\phi_d\rangle \times\psi_{\alpha_n}(\vec{k}_1)\psi_{AP}(\xi_p,\vec{k}_i)\,, \tag{9}$$

where $\phi_d$ denotes the intrinsic wave function of the deuteron. In the initial state it represents the deuteronlike correlation between neutron and proton in the nucleus. $\vec{K}$ is the momentum vector associated with the center-of-mass motion of the *np* pair in the nucleus $A$. It is defined by $\vec{K}=\vec{k}_1+\vec{k}_i$. Owing to momentum conservation the transition matrix $\langle T_p\rangle$ in Eq. (9) gets factorized to

$$\langle \vec{k}'_i,\vec{k}'_d\phi_d \mid T_p \mid \vec{k}'_p,\vec{K}\phi_d\rangle=\delta(k'_i+\vec{k}'_d-\vec{k}'_p-\vec{K})\langle \vec{\alpha}' \mid T_{pd}\mid \vec{\alpha}\rangle\,, \tag{10}$$

where $\vec{\alpha}$ and $\vec{\alpha}'$ are the relative proton-deuteron momenta before and after the collision and are defined as

$$\vec{\alpha}=(m_p\vec{K}-m_d\vec{k}'_p)/(m_p+m_d)\,,\qquad \vec{\alpha}'=(m_p\vec{k}'_d-m_d\vec{k}'_i)/(m_p+m_d)\,. \tag{11}$$

The matrix element $\langle T_{pd}\rangle$ may be identified as describing the *pd* scattering from momentum state $\vec{\alpha}$ to $\vec{\alpha}'$. As such this matrix element is completely offshell and thus cannot be related to the measured free *pd* scattering cross section. However, considering that the off-shell effect introducing sources like the binding energy of participating nucleons and the distorting potentials at high energies are much smaller than the incident energy, we approximate the $\langle T_{pd}\rangle$ by its on-shell value and write

$$\langle \vec{\alpha}' \mid T_{pd}\mid \vec{\alpha}\rangle\approx T_{pd}(\epsilon,\theta_p^{\text{c.m.}})\,, \tag{12}$$

where the relative energy $\epsilon$ and the scattering angle $\theta_p^{\text{c.m.}}$, in the *pd* center of mass are given by

$$\epsilon=\hbar^2\alpha^2/2\mu_{pd};\quad \cos\theta_p^{\text{c.m.}}=\hat{\alpha}'\cdot\hat{\alpha}\,. \tag{13}$$

Here $\mu_{pd}$ is the reduced mass for the proton and deuteron system. If, in the evaluation of $\epsilon$ and $\theta_p^{\text{c.m.}}$, we average over the directions of the bound particles, the expressions for them get simplified to

$$\epsilon\approx\frac{\hbar^2}{2\mu_{pd}}\left[\frac{K^2}{9}+\tfrac{4}{9}k'^2_p\right], \tag{14}$$

$$\cos(\pi-\theta_p^{\text{c.m.}})\approx\cos\theta_d\Big/\left[\left[1+\frac{1}{4}\frac{K^2}{k'^2_p}\right]\left[1+4\frac{k'^2_i}{k'^2_d}\right]\right], \tag{15}$$

where $\theta_d$ is the angle of the outgoing deuteron in the $p-A$ center-of-mass system in the $A(p,d)B$ reaction. In writing Eq. (15) we have assumed the straight line trajectories for the incoming proton and the outgoing deuteron and thus the angle between $\vec{k}'_d$ and $\vec{k}'_p$ is equated to the asymptotic scattering angle $\theta_d$. Furthermore, since the momentum of bound nucleons in the nucleus occurs, with significant probability, only up to about 200 MeV/$c$, $K^2$ and $k'^2_i$ in Eqs. (17) and (18) influence the value of $\epsilon$ and $\theta_p^{\text{c.m.}}$ only marginally. These variables, therefore, in Eqs. (14) and (15) can be replaced by their average values. With these observations the substitution of Eq. (10) into Eq. (9) and integration over $\vec{k}'_i$ factorizes $G$ to

$$G(\vec{k}'_d,\vec{k}'_p)=T_{pd}(\epsilon,\theta_p^{\text{c.m.}})S_{BA}^{1/2}(\alpha_n)\times\sum_i\int d\xi_p d\vec{k}_1 d\vec{k}_i\psi^*_{BP}(\xi_p,\vec{K}+\vec{Q}')\times\psi_{AP}(\xi_p,\vec{k}_i)\psi_{\alpha_n}(\vec{k}_1)\,, \tag{16}$$

where $\vec{Q}'$ is the momentum transfer and is given by

$$\vec{Q}'=\vec{k}'_p-\vec{k}'_d\,. \tag{17}$$

If the target nucleus is not heavy enough to justify the neglect of terms of the order $A^{-1}$ expression (17) for $\vec{Q}'$ gets modified to

$$\vec{Q}'=\alpha\vec{k}'_p-\beta\vec{k}'_d\,, \tag{18}$$

where

$$\alpha=1-2/A;\quad \beta=1-1/(A-1)\,.$$

In order to put expression (16) in compact form we introduce the form factor $\rho^p_{BA}$ for protons, which is defined as

$$\rho^p_{BA}(\vec{k}_1+\vec{Q}')=\sum_i\int d\vec{k}_i d\xi_p\psi^*_{BP}(\xi_p,\vec{K}+\vec{Q}')\times\psi_{AP}(\xi_p,\vec{k}_i)\,, \tag{19}$$

where $\rho^p_{BA}$ is normalized such that $\rho^p_{BP}(0)=Z$, the number of protons in the target nucleus. This form factor could be elastic or inelastic. With this form factor Eq. (16) becomes

$$G(\vec{k}'_d,\vec{k}'_p)=T_{pd}(\epsilon,\theta_p^{\text{c.m.}})S_{BA}^{1/2}(\alpha_n)\times\int d\vec{k}_1\rho^p_{BA}(\vec{k}_1+\vec{Q}')\psi_{\alpha_n}(\vec{k}_1)\,. \tag{20}$$

On substituting expression (20) for $G$ in Eq. (4) for the transition matrix, $T_{BA}$, $T_{pd}$, due to its dependence on $\vec{k}'_p$ and $\vec{k}'_d$ [Eqs. (14) and (15)], still remains entangled with the distorted waves. However, if we notice that the depth of the real part of the optical potential at intermediate energies, say between 300 MeV and 1 GeV for $^{12}$C, varies between $-5$ MeV and $+20$ MeV, we can neglect the effect of dispersion in $T_{pd}$. Or we can replace $k_p'^2$ and $k_d'^2$ in Eqs. (14) and (15) by some typical local values. With this assumption the transition matrix $T_{BA}$ in Eq. (4) gets expressed as

$$T_{BA}(\vec{Q})=T_{pd}(\epsilon,\theta_p^{\text{c.m.}})S_{BA}^{1/2}(\alpha_n)F^{BA}_{\alpha_n}(\vec{k}_d,\vec{k}_p)\,, \tag{21}$$

where

$$F^{BA}_{\alpha_n}(\vec{k}_d,\vec{k}_p)=\int d\vec{k}'_p d\vec{k}'_d\chi^*_{\vec{k}'_d}(\vec{k}'_d)\times\left\{\int d\vec{k}_1\rho^p_{BA}(\vec{k}_1+\vec{Q}')\psi_{\alpha_n}(\vec{k}_1)\right\}\times\chi^+_{\vec{k}'_p}(\vec{k}'_p) \tag{22}$$

and $\vec{Q}$ is the momentum transfer and is defined analogous to Eq. (18), i.e.,

$$\vec{Q}=\alpha\vec{k}_p-\beta\vec{k}_d\,. \tag{23}$$

Correspondingly the expression for the cross section for the neutron from a given orbital "$\alpha_n$," after summing over the spin projections, becomes

$$\frac{d\sigma}{d\Omega}=F_K\,\overline{|T_{pd}(\epsilon,\theta_p^{\text{c.m.}})|^2}\times\sum_m\frac{S_{BA}(lj)}{(2l+1)}|F^{BA}_{jlm}(Q)|^2\,, \tag{24}$$

where we have identified the orbital "$\alpha_n$" with the shell model orbital "$jlm$." The matrix element $|T_{pd}|^2$ can be related to the experimentally measured free $pd$ scattering cross section by

$$\overline{|T_{pd}(\epsilon,\theta_p^{\text{c.m.}})|^2}=\frac{9}{4}\frac{(2\pi)^2\hbar^4}{m_N{}^2}\frac{\alpha}{\alpha'}\sigma_{pd}\times(\epsilon_L,\theta_p^{\text{c.m.}})\,, \tag{25}$$

where $m_N$ is the nucleon mass and $\sigma_{pd}$ is the free $pd$ cross section in its center of mass at laboratory energy $\epsilon_L$ and center of mass scattering angle $\theta_p^{\text{c.m.}}$. $\theta_p^{\text{c.m.}}$, as given by Eq. (15), is related to $\theta_d$ and corresponds to backward scattering. $\epsilon_L$ is related to $\epsilon$ [Eq. (14)] by (ignoring terms of the order of $A^{-2}$)

$$\epsilon_L=\tfrac{3}{2}\epsilon\approx\frac{A}{A+2}T_p-\frac{A}{A+1}U(T_p)+\frac{A-1}{2(A+1)}\bar{\epsilon}\,, \tag{26}$$

where $T_p$ is the laboratory energy of proton in $A(p,d)B$ reaction and $U(T_p)$ is some typical value of the real part of the optical potential. $\bar{\epsilon}=\bar{K}^2/4m$, where $\bar{K}^2$ is the average value of $K^2$, and can be obtained from the following or any equivalent relation of average momentum of a group of $N$ nucleons in a nucleus with $A$ nucleons[13]

$$\bar{K}^2=\frac{N(A-N)}{A-1}\tfrac{3}{5}k_F{}^2\,, \tag{27}$$

where $k_F$ is the Fermi momentum. The value of $\bar{\epsilon}$ could be around 25 MeV.

Using the following transformations for $\psi(k_1)$, $\rho^p_{BA}(q)$, and the distorted waves, expression (22) for $F^{BA}_n(Q)$ can also be written in the configuration space

$$\psi(\vec{k}_1)=(2\pi)^{-3/2}\int e^{-i\vec{k}_1\cdot\vec{r}}\psi(\vec{r})d\vec{r}\,, \tag{28}$$

$$\rho^p_{BA}(\vec{q})=\int e^{-i\vec{q}\cdot\vec{r}}\rho^p_{BA}(\vec{r})d\vec{r}\,, \tag{29}$$

$$\chi_{\vec{k}}(\vec{k}')=(2\pi)^{-3}\int e^{-i\vec{k}'\cdot\vec{r}}\chi_{\vec{k}}(\vec{r})d\vec{r}\,, \tag{30}$$

where $\psi(r)$ is normalized to unity and $\chi_{\vec{k}}(r)$, in the plane wave, takes the form $\exp(i\vec{k}\cdot\vec{r})$. $F(Q)$, then, in $r$ space becomes

$$F^{BA}_{jlm}(\vec{Q})=(2\pi)^{3/2}\int d\vec{r}\chi^*_{\vec{k}_d}(\beta\vec{r})\chi^+_{\vec{k}_p}(\alpha\vec{r})\times\psi_{jlm}(\vec{r})\rho^p_{BA}(\vec{r})\,. \tag{31}$$

Since in the intermediate energy range the eikonal approximation is expected to be a good approximation, the distorted waves in Eq. (31) are written as

$$\chi^*_{\vec{k}_d}(\beta\vec{r})\chi^+_{\vec{k}_p}(\alpha\vec{r})=e^{i\vec{Q}\cdot\vec{r}}D_{\vec{k}_d}(\beta\vec{r})D_{\vec{k}_p}(\alpha\vec{r})\,, \tag{32}$$

where $D$'s are the distorting functions. They are defined by

$$D_{\vec{k}_d}(\beta\vec{r})=\exp\left[-\frac{iE_d}{\hbar^2c^2k_d}\times\int_0^\infty V_d(|\beta\vec{r}+\hat{k}_d s|)ds\right]\,, \tag{33}$$

$$D_{\vec{k}_p}(\alpha\vec{r})=\exp\left[-\frac{iE_p}{\hbar^2c^2k_p}\times\int_0^\infty V_p(|\alpha\vec{r}-\hat{k}_p s|)ds\right]. \quad (34)$$

Since in the $A(p,d)B$ experiments the deuterons are measured near the forward directions ($<30°$), for the evaluation of $D_{\vec{k}_d}$ we approximate the deuteron path length in the nucleus by that parallel to $\vec{k}_p$. With this approximation and taking $z$ axis parallel to $\vec{k}_p$, the distortion functions do not depend upon the azimuthal angle $\varphi$. Thus one gets

$$F^{BA}_{jlm}(Q)=(2\pi)^{5/2}(-1)^m \times\int b\,db\,dz\,e^{iQ_{\|}z}J_m(Q_\perp b)D_{\vec{k}d}(\beta b,\beta z)D_{\vec{k}_p}(\alpha b,\alpha z)\rho^p_{BA}(b,z)R_{nlj}(b,z)C_{lm}(\theta)\,, \quad (35)$$

where $J_m$ is the cylindrical Bessel function. $Q_{\|}$ and $Q_\perp$ are the longitudinal and transverse components of the momemtum transfer $\vec{Q}$, respectively. $R_{nlj}$ is the radial part of the neutron wave function and $C_{lm}$ is defined as

$$Y_{lm}(\theta,\varphi)=C_{lm}(\theta)e^{im\varphi} \quad (36)$$

with

$$\theta=\tan^{-1}(b/z)\,.$$

## III. RESULTS AND DISCUSSION

The experimental data on the $(p,d)$ reaction exist at 700 MeV on $^{12}$C and 800 MeV on $^{12,13}$C and $^{40}$Ca. Data are also available at lower energies (200–500 MeV) on $^4$He, Li, and at a fixed angle (22.5°) on $^{13}$C (Refs. 2–4). In this paper we have mainly done calculations for $^{12}$C and some results are obtained for $^{40}$Ca. As regards the input information needed for the calculations, the situation is not very good. The proton optical potentials are taken from the following sources:

(i) Batty and Phillips, for the energy range 200–800 MeV and 1 GeV (Ref. 14);

(ii) Blanpied *et al.*, for 800 MeV on $^{12}$C (Ref. 15);

(iii) Meyer *et al.*, for 200 MeV on $^{12}$C (Ref. 16);

(iv) Abdul Jalil *et al.*, between 100–200 MeV on $^{12}$C (Ref. 17).

For the deuteron optical potential little information exists. In view of this we have employed the phenomenological deuteron optical potential as extracted from the analyses of the elastic scattering data on $^{16}$O$(d,d)$ at 698 MeV by Shepard and Rost.[7] Alternatively we have constructed the deuteron optical potential by summing those for the proton and neutron at half the deuteron energy. This approximation should be alright for the real part of the potential. The imaginary part ($W_d$), however, would be underestimated as this prescription does not include the deuteron breakup channel. As a first attempt to understand the gross features of the $(p,d)$ data in the quasideuteron model this choice of optical potential should be enough. For the same reason the calculations are done only for the transition to the ground state of the residual nucleus. For the density matrix in Eq. (35) we have employed the groundstate charge density. In this paper we have not done any detailed investigations about the nuclear structure aspect, like any possibility of an inelastic contribution of the proton core to the ground-state transition. If it does contribute, the magnitude of the cross section may change. For $^{12}$C the elastic charge density is parametrized as

$$\rho(r)=\rho_0[1+ar^2/b^2]e^{-r^2/b^2}\,, \quad (37)$$

with

$$\rho_0=\frac{2Z/b^3}{\pi^{3/2}(2+3a)}\,. \quad (38)$$

For $^{40}$Ca it is written as

$$\rho(r)=\rho_0(1+ar^2/b^2)/[1+e^{(r-b/a)}] \quad (39)$$

with

$$\rho_0=Z\left\{\frac{4\pi}{3}b\left[(b^2+\pi^2c^2)+\frac{a}{5b^2}(3b^4+10\pi^2c^2b^2+7\pi^4c^4)\right]\right\}^{-1}. \quad (40)$$

The parameters, $a$, $b$, $c$, which fit the elastic electron scattering data, are taken from De Jager *et al.*[18] For $^{12}$C, $a=1.247$ and $b=1.649$ fm. For $^{40}$Ca, $a=-0.102$, $b=3.661$ fm, and $c=0.594$ fm. The neutron wave functions in the nucleus are generated in a Woods-Saxon potential whose parameters are taken from Elton and Swift.[19] These parameters are found to fit the elastic electron scattering and the $(p,2p)$ and $(e,e'p)$ data.[20] The

calculations were also done using the bound-state wave functions of Negele.[21] However, it was observed that the predictions from these two classes of wave functions do not differ significantly. This is understandable as these two wave functions differ only in the region of high momentum components which the quasideuteron model, due to the presence of proton density matrix in Eq. (35), does not necessarily sample.

The free *pd*-scattering angular distribution at backward angles exists at 598 MeV,[22] 1 GeV,[23] and in some restricted angular region at some other energies.[24] For $\theta_p \geq 175°$, of course, a complete documentation is given in a paper by Bonner *et al.*[25] Using all this available information we have interpolated as judiciously as possible the free *pd* cross section required in our calculations.

In Figs. 2 and 3 using the spectroscopic factor of 3, we show the calculated angular distributions for $^{12}$C at 800 and 700 MeV. The 800-MeV data are from Ref. 3 and the 700 MeV data from Baker *et al.*[2] The dashed curves in both figures, which have normalizations of $\frac{1}{9}$ at 800 MeV and $\frac{1}{13}$ at 700 MeV, use the 800-MeV proton optical potential of Blanpied *et al.*[15] and the 698-MeV deuteron optical potential for $^{16}$O. The solid curves are obtained using the deuteron optical potentials constructed

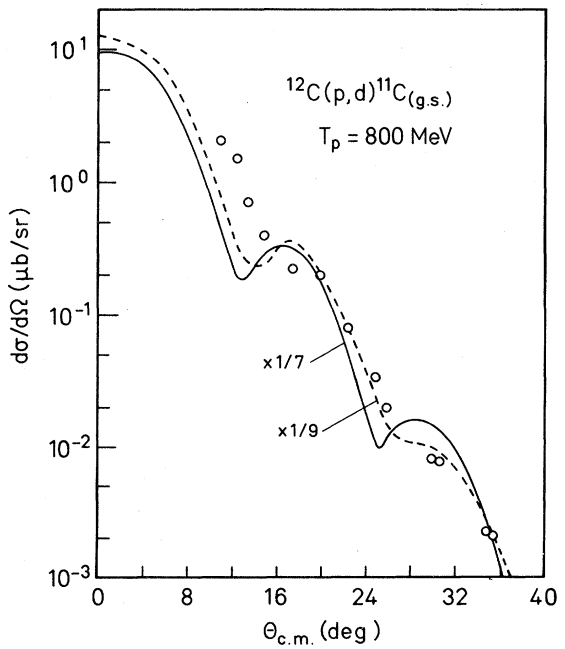


FIG. 2. Differential cross section for the reaction $^{12}$C$(p,d)^{11}$C(g.s.) at $T_p = 800$ MeV. The two curves correspond to two choices of the optical potentials.

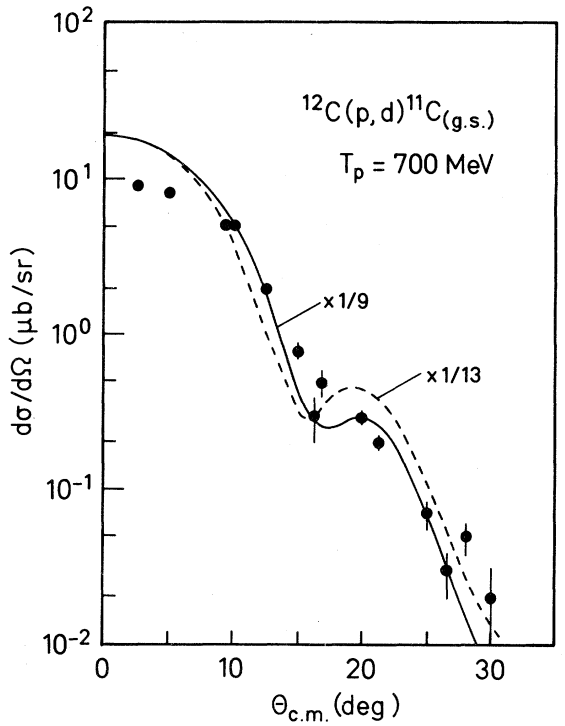


FIG. 3. Same as Fig. 3 except that $T_p = 700$ MeV.

from the nucleon optical potentials due to Batty.[14] The proton optical potential at 800 MeV is retained as that in the dashed curve while at 700 MeV it has been taken from Batty.[14] The normalization factors, as shown in the figures, are $\frac{1}{7}$ at 800 MeV and $\frac{1}{9}$ at 700 MeV. As we see from these figures the shapes of the measured distributions, are reproduced well. The magnitudes are, of course, overestimated by about an order of magnitude. This overestimation of the cross section may be remedied by employing better nuclear structure information about $^{12}$C and better known optical potentials. For example, as regards the nuclear structure, it is known that the ground state of the $^{12}$C nucleus is deformed. The deuteron optical potentials constructed from summing the neutron and proton potentials at half the deuteron energy (which we use extensively in this paper), as mentioned earlier, do not include the breakup channel. The imaginary part of the actual potential should therefore be larger than that coming from this prescription. Since the probability for the breakup of the deuteron becomes larger at higher energies, this increase in the imaginary part of the potential ($W_d$) may be substantial. In order to see the effect of increased $W_d$ we calculated the cross section at 700 MeV for the forward angle by making $W_d$ one and

a half ($\frac{3}{2}$) and two times that used in the solid curve. The cross section correspondingly gets reduced by a factor of about 1.5 and 2.5, respectively.

In order to see the variation of the cross section with the incident proton energy, we show in Fig. 4 the cross section at fixed deuteron angles, $\theta_d = 2.5°$ and 22.5°, as a function of $T_p$ from 200 MeV to 1 GeV. The deuteron optical potentials are constructed from the nucleon potentials. The nucleon potentials themselves are taken for above 250 MeV from Batty[14] and for below 250 MeV from Meyer *et al.*[16] and Abdul Jalil *et al.*[17] The experimental data on $^{12}$C below 700 MeV do not exist. However, they do exist on $^{13}$C at $\theta_d = 22.5°$ (Ref. 4). Therefore from 200 to 500 MeV we have shown in the figure the data for $^{13}$C. They are, of course, renormalized corresponding to the spectroscopic factor 3 in the $^{12}$C transition. The spectroscopic factor for $^{13}$C $(p,d)^{12}$C is taken as unity and the difference due to the $1P_{1/2}$ and $1P_{3/2}$ neutron wave functions is ignored. It is very impressive to observe that the trend of the measured cross section is remarkably well reduced. The bumps in the cross section between 300–600 MeV arise due to the similar plateau in the *pd* scattering data at backward angles. At 22.5° it gets more pronounced as the node of the structure factor $F_n^{BA}(Q)$ [Eq. (22)] also occurs in the same region.

In the literature[4] one has also plotted the measured cross section as a function of the momentum transfer $Q$. It is found that with respect to this variable the cross section falls off rapidly and can be fitted by an exponential function $\sigma = \sigma_0 \exp(-Q/Q_0)$, with $Q_0 \sim 47$ MeV/$c$ for carbon isotopes. From our calculations at 400, 600, 800, and 1000 MeV incident energies, in Fig. 5 we also show the cross section for $^{12}$C as a function of $Q$. As we see, like the experiments, the general falloff of the calculated cross section in the momentum range 300–800 MeV/$c$ also follows the exponential

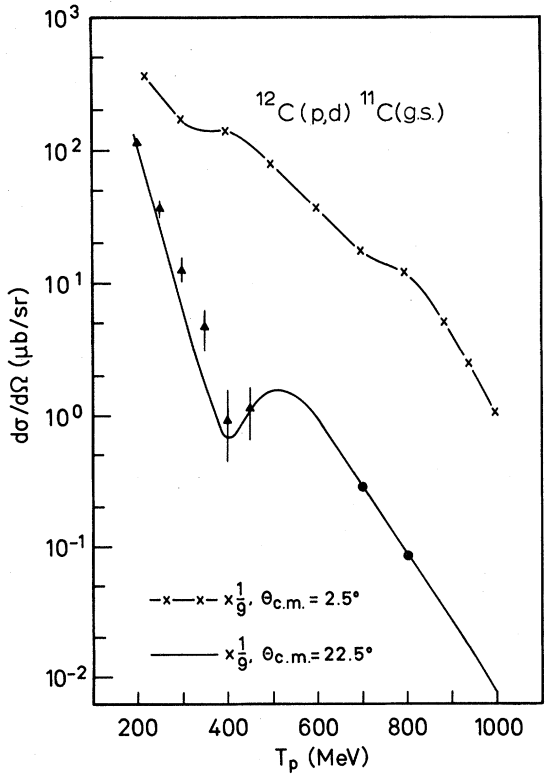


FIG. 4. Variation of the cross section for $^{12}$C$(p,d)^{11}$C(g.s.) at $\theta_d = 2.5°$ and 22.5° versus the incident proton energy $T_p$. The ▲ data are the $^{13}$C$(p,d)^{12}$C(g.s.) data renormalized corresponding to the $^{12}$C$(p,d)$ $^{11}$C(g.s.) spectroscopic factor (3). Other data are for $^{12}$C.

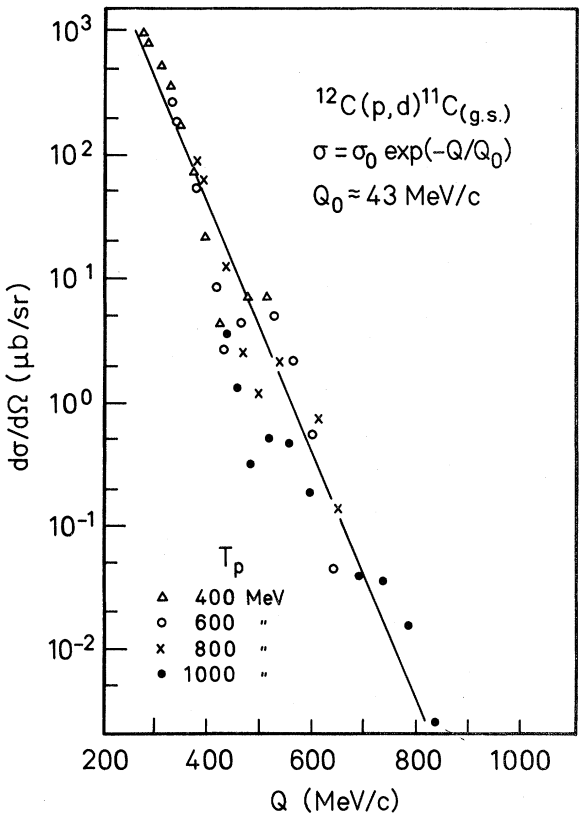


FIG. 5. Calculated cross section versus momentum transfer $Q$ at 400, 600, 800, and 1000 MeV incident energies. The continuous line with the slope parameter $Q_0 \sim 43$ MeV/$c$ is drawn to show the trend of the falloff of the cross section. The experimental data, not shown in the figure (Ref. 4), also show the similar behavior with $Q_0 \sim 46$ MeV/$c$.

behavior with $Q_0 \sim 43$ MeV/$c$. Also, comparing these distorted wave results with our corresponding plane-wave results (shown in Fig. 6) this general behavior of the cross section with respect to $Q$ does not change much due to distortion. Because of this observation, in Fig. 6 (right-hand curve), from our calculation at 400, 600, 800, and 1000 MeV, we also show the plane-wave results for $^{40}$Ca $(p,d)^{39}$Ca(g.s.) as a function of $Q$. Like $^{12}$C, these results also follow the exponential falloff and interestingly enough have approximately the same shaped parameter (i.e., $Q_0 \sim 43$ MeV/$c$). Considering that the $^{12}$C and $^{40}$Ca nuclei involve completely different neutron shells ($1p$ in $^{12}$C and $1d$ in $^{40}$Ca), this observation is a little surprising as well as interesting. At present it is not quite clear to us as what real significance should be attached to this observation. It, however, appears that, since in the present model the net falloff of the cross section with $Q$ arises due to the combined decrease of the structure factor $F_{\alpha_n}(Q)$ and the free $pd$ scattering cross section, any difference in $F_{\alpha_n}(Q)$ due to different $\alpha_n$ is smoothed out by the latter factor. Thus the net result (apart from the magnitude) does not depend very much on the target nucleus.

As mentioned earlier the experimental data are also available at 800 MeV on $^{40}$Ca. The inspection of the experimental data on $^{12}$C and $^{40}$Ca itself reveals that relative to $^{12}$C the cross section in $^{40}$Ca comes down by a factor of about 40. Purely on the basis of distortion, it is not expected that such a reduction could be introduced. In fact, in the conventional pickup model DWBA calculation on $^{40}$Ca it has been found that apart from the reduction due to distortion one needs an additional factor of 30 to come near the experimental cross section.[3] With this background and the fact that the optical potentials for $^{40}$Ca are not known, we had a little hesitation in comparing our calculated results with the experiments. Nevertheless, the calculated angular distribution for $^{40}$Ca$(p,d)^{39}$Ca at 800 MeV is shown in Fig. 7. The spectroscopic factor is taken to be 3 and the optical potentials for the proton and deuteron are taken to be the same as those for $^{12}$C (for the proton from Blanpied *et al.*[15] and for the deuteron from Shepard-Rost[7]) except that the radius parameter is enhanced in proportion to $A^{1/3}$. Again the shape of the distribution is well reproduced. In comparison to $^{12}$C the magnitude requires an additional reduction by about a factor of 7.5.

In summary it may be concluded that the quasideuteron model discussed in this paper accounts very well for the gross features of the $(p,d)$ reaction at intermediate energies. The magnitudes of the cross sections for $^{12}$C, however, are overestimated by order of magnitude. Considering the

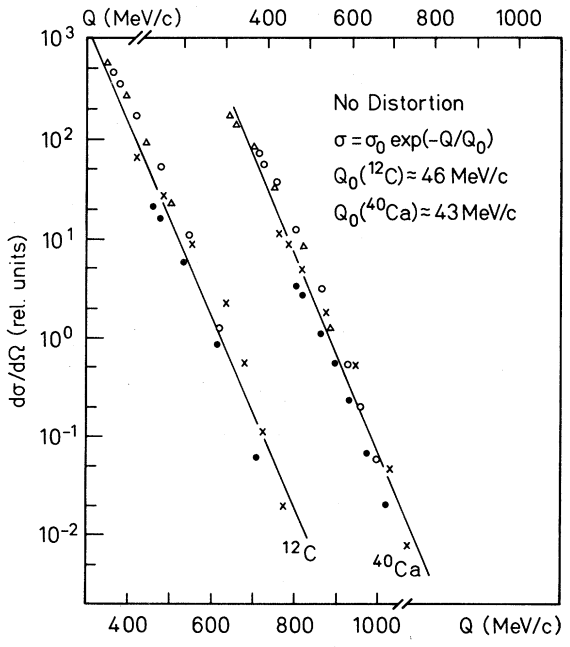


FIG. 6. Same as in Fig. 5 except that the distortions of proton and deuteron are switched off. The $Q$ scale for $^{40}$Ca is shown on the top, that for $^{12}$C on the bottom.

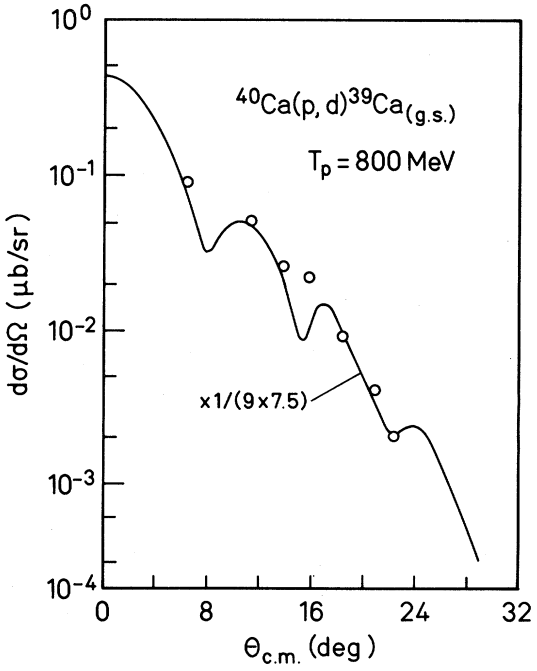


FIG. 7. Differential cross section for $^{40}$Ca$(p,d)^{39}$Ca(g.s.) at $T_p = 800$ MeV.

uncertainties in the input parameters and our reluctance, in this first attempt, to critically look into the nuclear structure effects, this at the present stage is not considered a source of great anxiety and disappointment.

## ACKNOWLEDGMENTS

In acknowledgment it is a great pleasure to thank Prof. J Hüfner for making several useful suggestions about preparing the manuscript. Thanks are also due to him and other members of the Institut für Theoretische Physik for their warm hospitality. The author also thanks Dr. R. C. Johnson of the University of Surrey for valuable discussions about the treatment of distortion. This work was partly supported by the German Federal Ministry of Research and Technology (BMFT).

---

*Permanent address: Nuclear Physics Division, Bhabha Atomic Research Centre, Bombay 40085, India.

[1]R. J. Philpott, W. T. Pinkston, and G. R. Satchler, Nucl. Phys. A119, 241 (1968).

[2]S. D. Baker *et al.*, Phys. Lett. 52B, 57 (1974).

[3]C. A. Whitten, Jr., Nucl. Phys. A335, 419 (1980).

[4]T. S. Bauer *et al.*, Phys. Lett. 67B, 265 (1977); Phys. Rev. C 21, 757 (1980); J. Källne *et al., ibid.* 21, 675 (1980); Phys. Rev. Lett. 41, 1638 (1978).

[5]K. Gottfried, Ann. Phys. (N.Y.) 21, 29 (1963).

[6]A. Boudard *et al.*, Phys. Rev. Lett. 46, 218 (1981); 47, 147 (1981); A. I. Yavin, Nucl. Phys. A374, 297 (1982).

[7]J. R. Shepard and E. Rost, Phys. Rev. Lett. 46, 1544 (1981).

[8]D. G. Measday and G. A. Miller, Annu. Rev. Nucl. Sci. 29, 121 (1979); R. E. Anderson *et al.*, Phys. Rev. C 23, 2616 (1981); H. A. Thiessen, Nucl. Phys. A335, 329 (1980).

[9]C. Wilkin, J. Phys. G 6, 69 (1980).

[10]N. S. Craigie and C. Wilkin, Nucl. Phys. B14, 477 (1969); V. M. Kolybasov and N. Ya. Smorodinskaya, Yad. Fiz. 17, 1211 (1973) [Sov. J. Nucl. Phys. 17, 630 (1973)].

[11]B. Schoch, Phys. Rev. Lett. 41, 80 (1978); H. W. Fearing, Phys. Rev. C 11, 1210 (1975); 11, 1493 (1975).

[12]E. Hadjimichael, S. N. Yang, and G. E. Brown, Phys. Lett. 39B, 594 (1972).

[13]A. S. Goldhaber, Phys. Lett. 53B, 306 (1974).

[14]C. J. Batty, Nucl. Phys. 23, 562 (1961); G. C. Phillips, in *Few Body Problems, Light Nuclei and Nuclear Interaction, Brela, Yugoslavia—1967,* edited by G. Paic and I. Slaus (Gordon and Breach, New York), p. 701.

[15]G. S. Blanpied *et al.*, Phys. Rev. C 23, 2599 (1981).

[16]H. O. Meyer *et al.*, Phys. Rev. C 24, 1782 (1981).

[17]Abdul Jalil and D. F. Jackson, J. Phys. G 5, 1699 (1979).

[18]C. W. De Jager, H. De Vries, and C. De Vries, At. Data Nucl. Data Tables 14, 479 (1974).

[19]L. R. B. Elton and A. Swift, Nucl. Phys. A94, 52 (1967).

[20]R. Shanta and B. K. Jain, Nucl. Phys. A175, 417 (1971).

[21]J. W. Negele, Phys. Rev. C 1, 1260 (1970).

[22]J. Vincent *et al.*, Phys. Rev. Lett. 24, 236 (1970).

[23]G. Bennett *et al.*, Phys. Rev. Lett. 19, 387 (1967); E. Coleman *et al., ibid.* 16, 761 (1966).

[24]J. C. Alder, R. M. Heinz, O. E. Overseth, and D. E. Pellett, Phys. Rev. C 6, 2010 (1972); G. A. Leskin, Zh. Eksp. Teor. Fiz. 5, 440 (1957) [Sov. Phys.—JETP 5, 371 (1957)].

[25]B. E. Bonner *et al.*, Phys. Rev. Lett. 39, 1253 (1977); J. E. Simons, in *High Energy Physics and Nuclear Structure—1975 (Sante Fe and Los Alamos),* Proceedings of the Sixth International Conference on High Energy Physics and Nuclear Structure, AIP Conf. Proc. No. 26, edited by D. E. Nagle *et al.* (AIP, New York, 1975), p. 103.